Self-consistent description of a spherically-symmetric gravitational collapse

Daniel R. Terno

Department of Physics & Astronomy, Macquarie University, Sydney, New South Wales 2109, Australia

(Received 16 June 2019; revised manuscript received 12 August 2019; published 10 December 2019)

In spherical symmetry, the total energy-momentum tensor near the apparent horizon is identified up to a single function of time from two assumptions: a trapped region forms at a finite time of a distant observer, and values of two curvature scalars are finite at its boundary. In general relativity, this energy-momentum tensor leads to the unique limiting form of the metric. The null energy condition is violated across the apparent horizon and is satisfied in the vicinity of the inner apparent horizon. As a result, homogenous collapse models cannot describe the formation of a black hole. Properties of matter change discontinuously immediately after formation of a trapped region. Absolute values of comoving density, pressure, and flux coincide at the apparent horizon. Thus, collapse of ideal fluids cannot lead to the formation of black holes. Moreover, these three quantities diverge at the expanding apparent horizon, producing a regular (i.e., finite curvature) firewall. This firewall is incompatible with quantum energy inequalities, implying that trapped regions, once formed at some finite time of a distant observer, cannot grow.

DOI: 10.1103/PhysRevD.100.124025

I. INTRODUCTION

Black holes (BHs) are envisaged as spacetime regions where gravity is so strong that nothing, not even light, can escape [1–3]. Mathematical black holes are solutions of the Einstein equations of general relativity (GR) [4–6]. The salient property of these solutions is the event horizon that separates the outside world from the black hole interior. Astrophysical black hole (ABH) candidates are massive compact dark objects. It is still not known how, when, and if at all they develop the distinctive features of the black holes of GR [7,8].

Quantum effects and uncertainty regarding the end result of the collapse [8–10] motivate investigations of exotic compact objects (ECOs) that do not lead to formation of an event horizon and/or singularity. Advances in instrumentation make studies of spacetime close to ABHs possible [11], focusing attention on the observational differences between ECO and conventional black holes [7,8,12–15].

Event horizons are global teleological entities that are in principle unobservable [3,7], and theoretical, numerical, and observational studies focus on other characteristics of BHs [16,17]. A trapped region is a domain where both ingoing and outgoing future-directed null geodesics emanating from a spacelike two-dimensional surface with spherical topology have negative expansion [4,16–18]. This local backward bending of light prevents communications with the outside world. The apparent horizon is the outer boundary of the trapped region [4,16].

Operationally relevant BH features should form at a finite time of a distant observer (Bob). As trapping of light is the essence of black holes [2], we formulate the assumption "a BH exists" as a statement that a trapped region have emerged at some finite time t_S of Bob. The simplest setting to investigate is a spherically-symmetric collapse, where the apparent horizon is unambiguously defined in all foliations that respect this symmetry [19]. The analysis of Refs. [20,21] produced explicit expressions for the energy-momentum tensor and the metric in the vicinity of expanding or contracting trapped regions. First, we briefly summarize the relevant results of Refs. [20,21] and then explore their implications.

II. GEOMETRY IN THE VICINITY OF THE APPARENT HORIZON

We assume validity of semiclassical gravity [22,23]. That means we use classical notions (horizons, trajectories, etc.) and describe dynamics via the Einstein equations where the standard (or modified) left-hand side is equated to the expectation value $T_{\mu\nu} = \langle \hat{T}_{\mu\nu} \rangle_\omega$ of the renormalized stress-energy tensor. The latter represents both the collapsing matter and the created excitations of the quantum fields, but we do not assume any specific field state ω.

Boundaries of the trapped region are required to be nonsingular, which is an established property of classical BH horizons. We implement this property by requiring that the scalars $\mathrm{T} := T^\mu_\mu$ and $\mathfrak{T} := T^{\mu\nu}T_{\mu\nu}$ are finite. This is only a necessary condition, and in principle further investigations of the resulting metric are required. However, in spherical symmetry, these two constraints are sufficient (see the Appendix A for details).

Hawking radiation is not assumed. On the contrary, the presence of the negative energy density that is described below is a consequence of the finite formation time of the apparent horizon and its regularity.

A general spherically symmetric metric in the Schwarzschild coordinates is given by

$$ds^2 = -e^{2h(t,r)}f(t,r)dt^2 + f(t,r)^{-1}dr^2 + r^2 d\Omega, \quad (1)$$

where r is the areal radius. The function $f(t,r) = 1 - C(t,r)/r$ is coordinate independent [19,24,25]. The Misner-Sharp mass [6,16,24] $C(t,r)$ is invariantly defined via

$$1 - C/r \coloneqq \partial_\mu r \partial^\mu r \equiv \nabla_\mu r \nabla^\mu r. \quad (2)$$

This is a gauge-independent equation for a scalar geometrically-defined quantity. On the other hand, the choice of r as one of the coordinates is a partial gauge fixing [19]. The function $h(t,r)$ plays the role of an integrating factor in transformation to, say, retarded or advanced coordinates. In the Schwarzschild spacetime, $C = 2M = \text{const}$ and $h = 0$.

Trapped regions exist only if the equation $f(t,r) = 0$ has a root [18]. For any foliation that respects spherical symmetry, the areal radius of the apparent horizon r_g is found [19,26] as a solution of

$$r_g = C(r_g). \quad (3)$$

This root (or, if there are several, the largest one) is the Schwarzschild radius $r_g(t)$ that identifies the apparent horizon in all such foliations. For example, in the metric (1), an outgoing radial null geodesic has a tangent vector,

$$l^\mu = (1, e^h f, 0, 0). \quad (4)$$

A nonzero coefficient $\kappa \neq 0$ in the parallel transport equation $l^\mu l^\nu{}_{;\mu} = \kappa l^\nu$ is a measure of nonaffinity of the geodesic parametrization. Expansion [4] of the congruence of such geodesics is

$$\theta_l = l^\mu{}_{;\mu} - \kappa = 2e^h(1 - C/r)/r. \quad (5)$$

This quantity indeed changes the sign as r crosses r_g.

The assumption of regularity results in the generic form of the energy-momentum tensor close to the apparent horizon. For $x \coloneqq r - r_g(t) \to 0$, its 2×2 block $a, b = t, r$ is

$$T_{ab} = \Xi(t)\begin{pmatrix} e^{2h} & se^h/f \\ se^h/f & 1/f^2 \end{pmatrix}, \quad T_{\hat{a}\hat{b}} = \frac{\Xi(t)}{f}\begin{pmatrix} 1 & s \\ s & 1 \end{pmatrix}, \quad (6)$$

for some function Ξ, and $s = \pm 1$, and the second expression is written in the orthonormal basis. This form of $T_{\mu\nu}$ was obtained in Ref. [20] without using the Einstein equations. Hence, it will hold in any metric theory, e.g., in $f(R)$ theories [15,27], in the vicinity of the hypersurfaces $f(t,r) = 0$.

From now on, we assume that dynamics is described by the standard Einstein equations. To produce real solutions with trapped regions at finite time t [20] (see Appendix A for details),

$$\Xi(t) = -\Upsilon^2(t) < 0 \quad (7)$$

must hold, where the function Υ is determined below. Here, $s = \pm 1$ corresponds to $r_g' \coloneqq dr_g/dt < 0$ and $r_g' > 0$, respectively. Then, the energy-momentum tensor of Eq. (6) violates the null energy condition (NEC) [4,28]: $T_{\hat{a}\hat{b}}k^{\hat{a}}k^{\hat{b}} < 0$ for a radial null vector $k^{\hat{a}} = (1, s, 0, 0)$.

The metric functions are given as power series in terms of x as [20]

$$C = r_g(t) - a(t)\sqrt{x} + \frac{1}{3}x \ldots. \quad (8)$$

and

$$h = -\ln\frac{\sqrt{x}}{\xi_0(t)} + \frac{4}{3a}\sqrt{x} + \cdots, \quad (9)$$

where $a^2 \coloneqq 16\pi\Upsilon^2 r_g^3$ and the higher-order terms in x depend on the higher-order terms in $T_{\mu\nu}$. The function $\xi_0(t)$ is determined by the choice of the time variable.

The function $\Upsilon(t) > 0$ is determined by the rate of change of the Schwarzschild radius,

$$r_g'/\xi_0 = \pm 4\sqrt{\pi}\Upsilon\sqrt{r_g} = \pm a/r_g. \quad (10)$$

In the case of a retreating Schwarzschild radius, $r_g'(t) < 0$, the metric is most conveniently written using the advanced null coordinate v,

$$dt = e^{-h}(dv + f^{-1}dr). \quad (11)$$

It takes the form of a pure ingoing Vaidya metric,

$$ds^2 = -(1 - C_+(v)/r)dv^2 + 2dvdr + r^2 d\Omega, \quad (12)$$

where $C_+(v) = C(t(v,r),r)$ is a decreasing function, $C_+' < 0$. If $r_g'(t) > 0$, geometry near the apparent horizon is described by a pure outgoing Vaidya metric

$$ds^2 = -(1 - C_-(u)/r)du^2 - 2dudr + r^2 d\Omega, \quad (13)$$

where $C_-{}'(u) > 0$.

Consistency of the Einstein equations allows only two types of the higher-order terms in the components T_{tt}, T^{rr}, and T_t^r [21]. In both cases, the higher-order terms in both h and C are monomials of higher half-integer powers of x (Appendix A).

For a macroscopic black hole ($r_g \gg 1$), the evaporation process is quasistationary. The previous analysis should

match the steady-state results that are obtained on a background of an eternal black hole in an asymptotically flat spacetime. The steady-state evaporation follows the law $r_g' = -\kappa/r_g^2$, where $\kappa \sim 10^{-3}$–10^{-4}, [6,25,29,30]. Hence [21],

$$\Upsilon \approx \frac{\sqrt{\kappa}}{2\sqrt{2\pi} r_g^2}, \qquad \xi_0 \approx 2\sqrt{\pi r_g^3}\Upsilon = \frac{1}{2}a. \tag{14}$$

III. PHYSICS IN THE VICINITY OF THE APPARENT HORIZON

Collapse models can be solved only if the matter content and equations of state are known. However, the very fact of formation of the apparent horizon allows us to obtain some information about its vicinity. Consider a radially infalling (not necessarily geodesic) observer Alice that is very close to r_g. Alice's 4-velocity $u_{\rm A}^\mu = (\dot{T}, \dot{R}, 0, 0)$ determines her time axis. For one of the spacelike directions, we take $n_\mu^{\rm A} = e^h(-\dot{R}, \dot{T}, 0, 0)$. The energy density and pressure in Alice's frame are always given by $\rho_{\rm A} \coloneqq T_{\mu\nu} u_{\rm A}^\mu u_{\rm A}^\nu$ and $p_{\rm A} \coloneqq T_{\mu\nu} n_{\rm A}^\mu n_{\rm A}^\nu$. Her 4-velocity is timelike, $u_{\rm A}^\mu u_{{\rm A}\mu} = -1$; hence,

$$\dot{T} = \frac{\sqrt{F + \dot{R}^2}}{e^H F}, \tag{15}$$

where $F = f(T(\tau), R(\tau))$ and $H = h(T, R)$.

This relationships leads to the comoving values of density and pressure close to the retreating r_g,

$$\rho_{\rm A}^< = p_{\rm A}^< = -\frac{(\dot{R} + \sqrt{F + \dot{R}^2})^2}{F^2}\Upsilon^2. \tag{16}$$

For $X \coloneqq R(\tau) - r_g(T(\tau)) \lesssim a^2$, the expansion of $\dot{T}$ results in small negative values,

$$\rho_{\rm A}^< = p_{\rm A}^< = -\frac{\Upsilon^2}{4\dot{R}^2} + \mathcal{O}(\sqrt{x}). \tag{17}$$

Using the metric of Eq. (12) that is valid on both sides of a contracting apparent horizon, we see that the NEC is violated in some neighborhood inside the trapped region as well.

However, in the case of the growing r_g, when $r_g' > 0$,

$$\rho_{\rm A}^> = p_{\rm A}^> = -\frac{(\dot{R} - \sqrt{F + \dot{R}^2})^2}{F^2}\Upsilon^2 + \mathcal{O}(F^{-1}), \tag{18}$$

giving a divergent expression,

$$\rho_{\rm A}^> = p_{\rm A}^> = -\frac{2\dot{R}^2\Upsilon^2}{F^2} + \mathcal{O}(F^{-1}), \tag{19}$$

in the vicinity of the apparent horizon, as $F^2 \approx a^2 X/r_g^2 \to 0$. The flux $\phi \coloneqq T_{\mu\nu} u_{\rm A}^\mu n_{\rm A}^\nu$ satisfies

$$\phi_{\rm A}^< = \rho_{\rm A}^<, \qquad \phi_{\rm A}^> = -\rho_{\rm A}^>, \tag{20}$$

at the crossing of the retreating and advancing apparent horizons, respectively.

These results show that an expanding trapped region should be accompanied by a firewall—a region of unbounded energy density, pressure, and flux—that is perceived by an infalling inertial observer. Unlike the firewall from the eponymous paradox that appears as a contradiction between four assumptions [9,31], here it is a consequence of regularity of an expanding apparent horizon and its finite formation time.

The comoving values of the matter variables are independent of the function $h(t, r)$. The divergence follows from the form of the energy-momentum tensor near r_g that is given by Eq. (6) and the opposite signs of T_{tt} and T_{tr}. Hence, our previous analysis indicates that this divergence occurs in all metric theories.

All the steps that result in the identification of the metric functions outside the Schwarzschild radius can be performed in the vicinity of the inner horizon. Then, the energy-momentum tensor again has the form of Eq. (6), but with $\Xi \to +\Theta^2$ for some $\Theta(t)$. The solution of the Einstein equations has a similar form, and for the inner horizon propagating toward the center, $r_{\rm in}' < 0$, we find that $\partial_t C > 0$ (and divergent, as r approaches $r_{\rm in}$ from below). Hence, $0 < T_t^r = +\Theta^2$. For a comoving observer Charlie that is overtaken by the inner horizon, the local density, pressure. and flux are

$$\rho_{\rm C} = p_{\rm C} = \phi_{\rm C} = +\frac{\Theta^2}{4\dot{r}_{\rm C}^2}. \tag{21}$$

A. Horizon crossing by test particles

A massive test particle will cross the apparent horizon when the gap [23,32]

$$X(\tau) \coloneqq R(\tau) - r_g(T(\tau)) \tag{22}$$

becomes zero. The crossing is prevented if for some $X > 0$ (and $r_g > 0$)

$$\dot{X} = \dot{R} - r_g'\dot{T} > 0. \tag{23}$$

An analogous expression holds for the outgoing Vaidya metric [23,32], but not for the ingoing Vaidya metric of (12) [21,33].

In the vicinity of the apparent horizon, $x \ll r_g$ and

$$\dot{T} \approx -\dot{R}e^{-H}/F. \tag{24}$$

Using Eqs. (8) and (9), we find that

$$\dot{X} = -\frac{(\dot{R}^2 - 4\pi r_g^2 \Upsilon^2)}{2|\dot{R}|\sqrt{\pi} r_g^{3/2}\Upsilon}\sqrt{X} + \mathcal{O}(X) \tag{25}$$

and see that if a test particle is in the vicinity of the apparent horizon, $X \ll a^2$, it will cross the horizon unless $|\dot{R}| < 2\sqrt{\pi} r_g \Upsilon \sim \sqrt{\kappa} \sim 0.01$. (For comparison, a free-falling particle starting at rest from infinity crosses the event horizon of a classical black hole with $\dot{R} = -3/4$). This difficulty of crossing the horizon for slow-moving test particles is consistent with the results of Ref. [34].

Using the leading higher-order terms in the metric functions (Appendix A) allows us to obtain terms of the order of X and $X^{3/2}$ in the expansion of $\dot{X}$. Their evaluation under the assumption of the quasistationary evaporation does not lead to qualitatively different conclusions.

The same analysis applies to massless test particles. In this case, the trajectory is most conveniently parametrized by $\lambda := -R$ [35], and one evaluates the derivative $dX/d\lambda$. Then, $\dot{R} \to dR/d\lambda \equiv -1$, and the apparent horizon is always crossed.

B. Horizon dynamics

A general spherically-symmetric metric in comoving coordinates (here, comoving means that fictitious freely-falling observers remain at fixed values of the spatial coordinates χ, θ, ϕ) is given by

$$ds^2 = -e^{2\lambda} d\bar{t}^2 + e^{2\psi} d\chi^2 + r^2 d\Omega^2, \tag{26}$$

where the areal radius $r(\bar{t}, \chi)$ and the functions $\lambda(\bar{t}, \chi)$ and $\psi(\bar{t}, \chi)$ are to be determined. For an observer at $\chi = \text{const}$, the proper time is given by $d\tau = e^{\lambda} d\bar{t}$, and the outward-pointing spacelike normal is $n_\mu = (0, e^{\psi}, 0, 0)$. Then, the comoving energy density, pressure, and flux are

$$\rho = -T^{\bar{t}}_{\bar{t}}, \qquad p = T^{\chi}_{\chi}, \qquad \phi = T^{\chi}_{\bar{t}} e^{\psi - \lambda}. \tag{27}$$

The Misner-Sharp mass $\mathscr{C}(\bar{t}, \chi)$ [defined via Eq. (2)] simplifies the Einstein equations [6,36]. In the metric (26), it is

$$\mathscr{C}(\bar{t}, \chi) = r(1 - e^{-2\psi}(\partial_\chi r)^2 + e^{-2\lambda}(\partial_{\bar{t}} r)^2), \tag{28}$$

and the three relevant Einstein equations are

$$-\frac{\partial_\chi \mathscr{C}}{r^2 \partial_\chi r} + \frac{2\partial_{\bar{t}} r e^{-2\lambda}}{r \partial_\chi r}(\partial_{\bar{t}}\partial_\chi r - \partial_{\bar{t}} r \partial_\chi \lambda - \partial_{\bar{t}}\psi \partial_\chi r) = -8\pi\rho, \tag{29}$$

$$-\frac{\partial_{\bar{t}} \mathscr{C}}{r^2 \partial_{\bar{t}} r} - \frac{2\partial_\chi r e^{-2\psi}}{r \partial_{\bar{t}} r}(\partial_{\bar{t}}\partial_\chi r - \partial_{\bar{t}} r \partial_\chi \lambda - \partial_{\bar{t}}\psi \partial_\chi r) = 8\pi p, \tag{30}$$

$$-\frac{2}{r}(\partial_{\bar{t}}\partial_\chi r - \partial_{\bar{t}} r \partial_\chi \lambda - \partial_{\bar{t}}\psi \partial_\chi r) = 8\pi\phi e^{\lambda + \psi}. \tag{31}$$

In contrast, the simplest models of gravitational collapse describe matter as a single perfect fluid with a comoving energy-momentum tensor,

$$T^{\mu}_{\nu} = \text{diagonal}(-\rho, p, p, p). \tag{32}$$

The absence of the flux term, $\phi \equiv 0$, leads via Eqs. (31) and (29) to a compact expression for the mass,

$$\mathscr{C}(\bar{t}, \chi) = 8\pi \int_0^{\chi} \rho r^2 r' d\chi \equiv C(t(\bar{t}, \chi), r(\bar{t}, \chi)), \tag{33}$$

where the last identity follows from the definition (2) evaluated in (t, r) coordinates with the metric of Eq. (1). However, at the apparent horizon, the flux is as important as pressure. Models that involve several nonideal fluids [37,38] should be used to describe the BH formation at finite Bob's time.

Violations of the NEC are bounded by quantum energy inequalities (QEIs) [39]. For spacetimes of small curvature, explicit expressions that bound time-averaged energy density for a geodesic observer were derived in Ref. [40]. For any Hadamard state ω and a sampling function $\mathfrak{f}(\tau)$ of compact support, negativity of the expectation value of the energy density $\rho = \langle \hat{T}_{\mu\nu} \rangle_\omega u^\mu u^\nu$ as seen by a geodesic observer that moves on a trajectory $\gamma(\tau)$ is bounded by

$$\int_\gamma \mathfrak{f}^2(\tau) \rho d\tau \geq -B(R, \mathfrak{f}, \gamma), \tag{34}$$

where $B > 0$ is a bounded function that depends on the trajectory, the Ricci scalar, and the sampling function [40].

Consider a growing apparent horizon, $r_g' > 0$. For a macroscopic BH, the curvature at the apparent horizon is low, and its radius does not appreciably change while Alice moves in the domain of validity of Eq. (19). Then, $\dot{X} \approx \dot{R}$, and given Alice's trajectory, we can choose $\mathfrak{f} \approx 1$ at the horizon crossing and $\mathfrak{f} \to 0$ within the NEC-violating domain. As the trajectory passes through $X_0 + r_g \to r_g$, the lhs of Eq. (34) behaves as

$$\int_\gamma \mathfrak{f}^2 \rho_{\mathrm{A}} d\tau \approx -\int_\gamma \frac{\dot{R}^2 d\tau}{8\pi r_g X} \approx \int_\gamma \frac{|\dot{R}| dX}{8\pi r_g X} \propto \log X_0 \to -\infty, \tag{35}$$

where we used $\dot{R} \sim \text{const}$. The rhs of Eq. (34) remains finite, and thus the QEI is violated. This violation indicates the apparent horizon cannot grow.

The values of ρ, p and ϕ are finite on the approach to the receding apparent horizon and the comoving metric remain regular. We can write Eq. (30) as

$$-\frac{e^{-\lambda}\partial_{\bar{t}} \mathscr{C}}{r^2 \dot{r}_\chi} + 8\pi \frac{\partial_\chi r}{\dot{r}_\chi} \phi e^{-\psi} = 8\pi p, \tag{36}$$

where $\dot{r}_\chi = \partial_{\bar{t}} r(\bar{t},\chi) d\bar{t}/d\tau < 0$, and the subscript χ indicates that the areal radius corresponds to a fixed comoving coordinate. From Eq. (8), it follows that both $\partial_t C$ and $\partial_r C$ diverge as $1/\sqrt{r-r_g}$. Using

$$\partial_{\bar{t}}\mathscr{C} = \partial_t C(t,r)\left.\frac{\partial t}{\partial \bar{t}}\right|_\chi + \partial_r C(t,r)\left.\frac{\partial r}{\partial \bar{t}}\right|_\chi = e^\lambda(\partial_t C(t,r)\dot{t}_\chi + \partial_r C(t,r)\dot{r}_\chi), \tag{37}$$

we find that $\partial_{\bar{t}}\mathscr{C}$ is finite only if $r_g'\dot{t}_\chi = \dot{r}_\chi$ as $r \to r_g$ (see Appendix B for details). However, Eqs. (24) and (10) imply precisely this relation, and thus no infinities are necessary to satisfy the Einstein equations (29)–(31).

IV. CONCLUSIONS

Trapped regions are physically relevant only if their formation time is finite. Hence, the only assumption we have made is the regularity of their boundary. We find that the NEC is violated in the vicinity of the apparent horizon and is satisfied in the vicinity of the inner apparent horizon. The form of the energy-momentum tensor that is given by Eq. (6) is the same in all metric theories of gravity, not only in GR. We expect that the NEC violation is also a necessary condition for the finite-time (according to Bob) formation of trapped regions in $f(R)$ theories, and we will investigate them in a future work.

Flux cannot be neglected in the vicinity of the apparent horizon. Hence, the collapse of a single ideal fluid (even allowing for violation of the NEC) cannot lead to formation of a black hole in finite time of a distant observer. In the classical homogeneous collapse, the first marginally trapped surface appears at the boundary of the collapsing body. However, the Misner-Sharp mass $\mathscr{C} > 0$, while the energy density is negative on both sides of the apparent horizon, and no system with a uniform density can form it.

Expanding the apparent horizon precipitates a firewall. Its divergent density, pressure, and flux do not lead to singularities but violate the QEI. Hence, either trapped regions cannot grow or the semiclassical analysis is inapplicable in their vicinity even if the curvature is small, as argued in Ref. [10]. It has a simple intuitive explanation: growth of r_g means growth of the BH mass. However, only the NEC-violating matter with negative energy density can cross the horizon, contributing to the mass decrease.

Infalling massive test particles may and massless test particles will cross the apparent horizon. However, the proverbial dropping of the Encyclopedia Britannica into a black hole that is followed by the alleged loss of information is impossible. A mandatory violation of the NEC in some vicinity of the apparent horizon is incompatible with preservation of the normal character of the perturbing matter. Hence, we have to investigate how perturbations by normal matter evolve and what happens to the perturbing material.

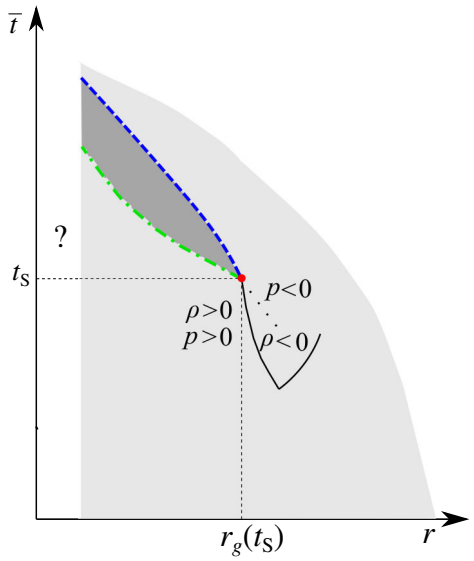

FIG. 1. Schematic structure of the early stages of the evolution of a trapped region (dark gray) if it forms at finite time t_S. Possible structures in the white patch near the time axis are not constrained by our considerations. The blue dashed line represents the apparent horizon, and the green dot-dashed line represents the inner apparent horizon. The first marginally trapped surface at $r = r_g(t_S)$ is marked as a red dot. Part of the region of negative density is outlined by a thin black line. Part of the boundary of the region of negative pressure is marked by the dotted black line. The shape and end points of the last two lines are not constrained by our considerations.

Propagating the limits of ρ, p, and ϕ back to t_S show that the first marginally trapped surface is a surface of discontinuity of the properties of collapsing matter, and a rather complicated diagram (Fig. 1) emerges. The trapped region forms at time t_S. At that moment the density in the central region of the collapsing body is still positive, $\rho > 0$ for $r \le r_{in}$. Causality and/or continuity arguments in the vicinity of $r_g(t_S)$ indicate that energy density becomes negative in some region close to $r_g(t_S)$ before formation of the horizons. The regions of negative pressure and density may not fully coincide, and their boundaries, as well as the possibility of discontinuity and shock waves inside the trapped region will be investigated in a future work.

ACKNOWLEDGMENTS

Useful discussions with Pisin Chen, Eleni Kontou, Robert Mann, Sebastian Murk, and Mark Wardle are gratefully acknowledged.

APPENDIX A: SOLUTIONS OF THE SPHERICALLY-SYMMETRIC EINSTEIN EQUATIONS NEAR AN APPARENT HORIZON

In spherical symmetry, the trace and the square of the energy-momentum tensor are

$$\mathrm{T} = -e^{-2h}T_{tt}/f + T^{rr}/f + 2T^{\theta}_{\theta}, \tag{A1}$$

$$\mathfrak{T} = -2\left(\frac{e^{-h}T^{r}_{t}}{f}\right)^2 + \left(\frac{e^{-2h}T_{tt}}{f}\right)^2 + \left(\frac{T^{rr}}{f}\right)^2 + 2(T^{\theta}_{\theta})^2. \tag{A2}$$

Assuming that T^{θ}_{θ} is finite (this can be proven in case of the standard GR), we obtain Eq. (6) as a generic case [20].

The Einstein equations that determine the functions h and C in the Schwarzschild coordinates are

$$G_{tt} = \frac{e^{2h}(r-C)\partial_r C}{r^3} = 8\pi T_{tt}, \tag{A3}$$

$$G^{r}_{t} = \frac{\partial_t C}{r^2} = 8\pi T^{r}_{t}, \tag{A4}$$

$$G^{rr} = \frac{(r-C)(-\partial_r C + 2(r-C)\partial_r h)}{r^3} = 8\pi T^{rr}. \tag{A5}$$

The requirement that the scalars T and $\mathfrak{T}$ are finite leads to the form of the energy-momentum tensor that is given by Eq. (10). The negative sign that results in violation of the NEC is necessary for having real solutions of the Einstein equations. This result should be compared with the conclusions of Sec. 9.2 of Ref. [4] that in general asymptotically flat spacetimes with an asymptotically predictable future the trapped surface cannot be visible from the future null infinity unless the weak energy condition is violated [4,5]. Here, we have considered only a spherically-symmetric setting, but without making assumptions about asymptotic structure of the spacetime [20].

Working in (u, r) or (v, r) coordinates provides the easiest way to establish that other curvature scalars are finite. In a general four-dimensional spacetime, there are 14 algebraically independent scalars that can be constructed from the Riemann tensor [41,42]. A convenient system of polynomial invariants consists of the Ricci scalar and a further 15 invariants [43]. A direct calculation [44] shows that for the metrics (12) and (13) all the invariants are identically zero, except for the two finite invariants that are constructed using the complex conjugate of the self-dual Weyl tensor [43],

$$\bar{C}_{\kappa\lambda\mu\nu} := \frac{1}{2}(C_{\kappa\lambda\mu\nu} + i^{*}C_{\kappa\lambda\mu\nu}), \tag{A6}$$

the invariants being

$$W_1 := \frac{1}{4}\bar{C}_{\kappa\lambda\mu\nu}\bar{C}^{\kappa\lambda\mu\nu}, \qquad W_2 := \frac{1}{4}\bar{C}_{\kappa\lambda\mu\nu}\bar{C}^{\mu\nu}{}_{\rho\sigma}\bar{C}^{\rho\sigma\kappa\lambda}. \tag{A7}$$

It is also easy to see that in this metric all the components of the Riemann tensor in the Vaidya coordinates [Eqs. (12) and (13)] are finite at $r = r_g$.

The higher-order terms in metric and energy momentum are of one of the two possible types [21]. The series expansion can be either regular,

$$T_{\hat{a}\hat{b}}f = -\Upsilon^2 + \sum_{n>1}\alpha^{(ab)}_{n}x^n, \tag{A8}$$

or regular singular,

$$T_{\hat{a}\hat{b}}f = -\Upsilon^2 + \sum_{n>1}\alpha^{(ab)}_{n}x^{n-1/2}. \tag{A9}$$

In both cases, the expansion follows the same pattern,

$$C(t, r_g + x) = r_g - a\sqrt{x} + \frac{1}{3}x + cx^{3/2} + gx^2 + \cdots \tag{A10}$$

and

$$h(t, r_g + x) = -\ln\frac{\sqrt{x}}{\xi_0} + k_2\sqrt{x} + k_3 x + k_4 x^{3/2} + \cdots, \tag{A11}$$

For a regular correction to $T_{\mu\nu}$ (we set $\alpha^{(tt)}_1 = \alpha_1, \alpha^{(tr)}_1 = \beta_1$, $\alpha^{(rr)}_1 = \gamma_1$), the terms of the metric functions that depend only on first-order corrections are

$$a = 4\sqrt{\pi}r_g^{3/2}\Upsilon, \tag{A12}$$

$$c = \frac{(36\pi\alpha_1 r_g^3 - 108\pi r_g^2\Upsilon^2 - 1)}{36\sqrt{\pi}r_g^{3/2}\Upsilon}, \tag{A13}$$

$$g = \frac{1}{540}\left(-\frac{36\alpha_1}{\Upsilon^2} + \frac{1}{\pi r_g^3\Upsilon^2} + \frac{108}{r_g}\right) \tag{A14}$$

and

$$k_2 = \frac{4}{3a}, \tag{A15}$$

$$k_3 = -\frac{3}{2r_g} - \frac{c}{a} + \frac{24\pi\alpha_1 r_g^3 + 24\pi\gamma_1 r_g^3 - 4}{6a^2}, \tag{A16}$$

$$k_4 = \frac{2(27a^2 g - 54ac - 16)}{81a^3} + \frac{2(-54a^2 + 144\pi\alpha_1 r_g^4 + 144\pi\gamma_1 r_g^4)}{81a^3 r_g}, \tag{A17}$$

where the functions $\xi_0(t)$ and $\Upsilon(t)$ are given by Eq. (14). Using Eq. (A4) and the conservation law $\nabla_\mu T^{\mu}_{\nu} = 0$ for $\nu = 0, 1$ allows us to obtain the recursive relations for the higher-order coefficients $\alpha^{(ab)}_n$ [21].

APPENDIX B: DETAILS OF EQ. (37)

Consider now the receding apparent horizon, $r_g' < 0$. The invariants T and $\mathfrak{T}$ are finite. In general, it does not imply that the metric functions are regular as $r \to r_g$: the functions $h(t,r)$ and $\partial_t C(t,r)$ diverge.

However, the Einstein equations imply

$$\partial_{\bar{t}}\mathscr{C} = \partial_t C(t,r)\left.\frac{\partial t}{\partial \bar{t}}\right|_\chi + \partial_r C(t,r)\left.\frac{\partial r}{\partial \bar{t}}\right|_\chi = e^\lambda(\partial_t C(t,r)\dot{t}_\chi + \partial_r C(t,r)\dot{r}_\chi). \tag{B1}$$

Here, we present in detail the analysis of Eq. (37). The two partial derivatives of $C(t,r)$ are

$$\partial_t C = \frac{2}{3}r_g' - a'\sqrt{r-r_g} + \frac{ar_g'}{2\sqrt{r-r_g}} \tag{B2}$$

and

$$\partial_r C = -\frac{ar_g'}{2\sqrt{r-r_g}} + \frac{1}{3}, \tag{B3}$$

where we omitted terms that approach zero as $r \to r_g$. For $\lambda > -\infty$ and $r_g' < 0$, Eq. (36) implies that the derivative $\partial_{\bar{t}}\mathscr{C}$ at r_g, is finite, i.e.,

$$\left|\lim_{r\to r_g}\left(\frac{ar_g'\dot{t}_\chi}{2\sqrt{r-r_g}} - \frac{a\dot{r}_\chi}{2\sqrt{r-r_g}}\right)\right| < \infty, \tag{B4}$$

only if

$$\lim_{r\to r_g}(r_g'\dot{t}_\chi - \dot{r}_\chi) = 0, \tag{B5}$$

i.e.,

$$r_g'\dot{t}_\chi \to \dot{r}_\chi, \tag{B6}$$

and the difference goes to zero faster than $\sqrt{x}$. Since the trajectory of a comoving particle is timelike, expansion of Eq. (10) results in

$$\dot{t}_\chi = -\frac{\dot{r}_\chi}{4\sqrt{\pi r_g}\xi_0\Upsilon} + \mathcal{O}(\sqrt{r_\chi - r_g}), \tag{B7}$$

which for a retreating apparent horizon implies Eq. (B6) via the consistency condition Eq. (10).

Using this relationship, we find

$$\lim_{r\to r_g} e^{-\lambda}\partial_{\bar{t}}\mathscr{C} = \frac{2}{3}r_g'\dot{t}_\chi + \frac{1}{3}\dot{r}_\chi = r_g'\dot{t}_\chi < 0, \tag{B8}$$

and the limiting form of Eq. (32) becomes

$$-\frac{1}{r_g^2} + 8\pi\frac{\partial_\chi r}{\dot{r}_\chi}\phi e^{-\psi} \approx 8\pi p, \tag{B9}$$

in the vicinity of the apparent horizon both for $r_g' < 0$ and $r_g' > 0$.

In the former case, $\phi \approx p < 0$. Using the approximation $r_g' = -\kappa/r_g^2$ to express the matter variable, Eq. (B9) becomes

$$-\frac{1}{r_g^2} + \frac{\partial_\chi r}{|\dot{r}_\chi^3|}\frac{\kappa e^{-\psi}}{r_g^4} \approx -\frac{\kappa}{r_g^4}, \tag{B10}$$

and the equation is satisfied if the function ψ reaches a large negative (but finite) value. In the latter case, $\phi \approx -p \propto 1/x > 0$, and Eq. (B9) becomes

$$\frac{\partial_\chi r}{\dot{r}_\chi}e^{-\psi} \approx -1. \tag{B11}$$

This relation indicates that unless the so-called shell crossing singularity [6] occurs, $\partial_\chi r = 0$, the function ψ should satisfy $\psi > -\infty$.

[1] J. Michell, Phil. Trans. R. Soc. A **74**, 35 (1784).
[2] E. Curiel, Nat. Astron. **3**, 27 (2019).
[3] M. Visser, Phys. Rev. D **90**, 127502 (2014).
[4] S. W. Hawking and G. F. R. Ellis, *The Large Scale Structure of Space-Time* (Cambridge University Press, Cambridge, England, 1973).
[5] V. P. Frolov and I. D. Novikov, *Black Holes: Basic Concepts and New Developments* (Kluwer, Dordrecht, Netherlands, 1998).
[6] C. Bambi, *Black Holes: A Laboratory for Testing Strong Gravity* (Springer, Singapore, 2017).
[7] V. Cardoso and P. Pani, Nat. Astron. **1**, 586 (2017); Living Rev. Relativity **22**, 4 (2019).
[8] L. Barack, V. Cardoso, S. Nissanke, and T. P. Sotiriou, Classical Quantum Gravity **36**, 143001 (2019).
[9] R. B. Mann, *Black Holes: Thermodynamics, Information, and Firewalls* (Springer, New York, 2015); D. Harlow, Rev. Mod. Phys. **88**, 015002 (2016).
[10] A. Ashtekar and M. Bojowald, Classical Quantum Gravity **22**, 3349 (2005); S. A. Hayward, Phys. Rev. Lett. **96**, 031103 (2006).

[11] Event Horizon Telescope Collaboration, Astrophys. J. Lett. **875**, L1 (2019).
[12] R. Carballo-Rubio, F. Di Filippo, S. Liberati, and M. Visser, Phys. Rev. D **98**, 124009 (2018).
[13] V. Cardoso, E. Franzin, and P. Pani, Phys. Rev. Lett. **116**, 171101 (2016).
[14] S. B. Giddings and D. Psaltis, Phys. Rev. D **97**, 084035 (2018); N. Oshita and N. Afshordi, Phys. Rev. D **99**, 044002 (2019).
[15] V. Cardoso, M. Kimura, A. Maselli, and L. Senatore, Phys. Rev. Lett. **121**, 251105 (2018).
[16] V. Faraoni, *Cosmological and Black Hole Apparent Horizons* (Springer, Heidelberg, 2015).
[17] *Astrophysical Black Holes*, edited by F. Haardt, V. Gorini, U. Moschella, A. Trever, and M. Colpi (Springer, Heidelberg, 2016).
[18] B. Krishnam, Quasi-local horizons, in *Springer Handbook of Spacetime*, edited by A. Ashtekar and V. Petkov (Springer, New York, 2014), p. 527.
[19] V. Faraoni, G. F. R. Ellis, J. T. Firouzjaee, A. Helou, and I. Musco, Phys. Rev. D **95**, 024008 (2017).
[20] V. Baccetti, R. B. Mann, S. Murk, and D. R. Terno, Phys. Rev. D **99**, 124014 (2019).
[21] V. Baccetti, S. Murk, and D. R. Terno, Phys. Rev. D **100**, 064054 (2019).
[22] A. Paranjape and T. Padmanabhan, Phys. Rev. D **80**, 044011 (2009).
[23] V. Baccetti, R. B. Mann, and D. R. Terno, Classical Quantum Gravity **35**, 185005 (2018).
[24] C. W. Misner and D. H. Sharp, Phys. Rev. **136**, B571 (1964).
[25] J. M. Bardeen, Phys. Rev. Lett. **46**, 382 (1981).
[26] W. C. Hernandez and C. W. Misner, Astrophys. J. **143**, 452 (1966).
[27] T. P. Sotiriou and V. Faraoni, Rev. Mod. Phys. **82**, 451 (2010); A. De Felice and S. Tsujikawa, Living Rev. Relativity, **13**, 3 (2010).
[28] P. Martín-Moruno and M. Visser, Classical and Semiclassical Energy Conditions, in *Wormholes, Warp Drives and Energy Conditions*, edited by F. N. S. Lobo (Springer, New York, 2017), p. 193.
[29] D. N. Page, Phys. Rev. D **13**, 198 (1976).
[30] R. Brout, S. Massar, R. Parentani, and P. Spindel, Phys. Rep. **260**, 329 (1995).
[31] A. Almheiri, D. Marolf, J. Polchinskib, and J. Sully, J. High Energy Phys. 02 (2013) 062.
[32] H. Kawai, Y. Matsuo, and Y. Yokokura, Int. J. Mod. Phys. A **28**, 1350050 (2013).
[33] B. Arderucio-Costa and W. G. Unruh, Phys. Rev. D **97**, 024005 (2018).
[34] L. C. Barbado, C. Barceló, L. J. Garay, and G. Jannes, J. High Energy Phys. 10 (**2016**) 161.
[35] R. B. Mann, I. Nagle, and D. R. Terno, Nucl. Phys. **B936**, 19 (2018).
[36] P. S. Joshi and D. Malafarina, Int. J. Mod. Phys. D **20**, 2641 (2011).
[37] M. Demianski and J. P. Lasota, Astrophys. Lett. **1**, 205 (1968); W. B. Bonnor, A. K. G. de Oliveira, and N. O. Santos, Phys. Rep. **181**, 269 (1989); L. S. M. Veneroni and M. F. A. da Silva, Int. J. Mod. Phys. D **28**, 1950034 (2019).
[38] L. Rezzolla and O. Zanotti, *Relativistic Hydrodynamics* (Oxford University Press, Oxford, 2013).
[39] C. J. Fewster, Quantum energy inequalties, in *Wormholes, Warp Drives and Energy Conditions*, edited by F. N. S. Lobo (Springer, New York, 2017), p. 215.
[40] E.-A. Kontou and K. D. Olum, Phys. Rev. D **91**, 104005 (2015).
[41] H. Stephani, D. Kramer, M. A. H. MacCallum, C. Hoenselaers, and E. Herlt, *Exact Solutions of Einsteins Field Equations*, 2nd ed. (Cambridge University Press, Cambridge, 2003), Chap. 9.
[42] E. Zakhary and C. B. G. McIntosh, Gen. Relativ. Gravit. **29**, 539 (1997).
[43] J. Carminati and R. G. McLenaghan, J. Math. Phys. (N.Y.) **32**, 3135 (1991).
[44] The calculations were performed using the symbolic tensor analysis package CCGRG, developed by A. Woszczyna *et al.*, http://library.wolfram.com/infocenter/MathSource/8848/.